

Higgs-boson production associated with a bottom quark at hadron colliders with SUSY-QCD corrections

Junjie Cao ^{a,b}, Guangping Gao ^b, Robert J. Oakes^c, Jin Min Yang ^b

^a CCAST(World Laboratory), P.O.Box 8730, Beijing 100080, China

^b Institute of Theoretical Physics, Academia Sinica, P.O.Box 2735, Beijing 100080, China

^c Department of Physics and Astronomy, Northwestern University, Evanston, IL 60208, USA

(November 3, 2018)

The Higgs boson production $pp (p\bar{p}) \rightarrow bh + X$ via $bg \rightarrow bh$ at hadron colliders, which may be an important channel for testing the bottom quark Yukawa coupling, is subject to large supersymmetric quantum corrections. In this work the one-loop SUSY-QCD corrections to this process are evaluated and are found to be quite sizable in some parameter space. We also study the behavior of the corrections in the limit of heavy SUSY masses and find the remnant effects of SUSY-QCD. These remnant effects, which are left over in the Higgs sector by the heavy sparticles, are found to be so sizable (for a light CP-odd Higgs and large $\tan\beta$) that they might be observable in the future experiment. The exploration of such remnant effects is important for probing SUSY, especially in case that the sparticles are too heavy (above TeV) to be directly discovered in future experiments.

14.80.Cp, 13.85.Qk, 12.60.Jv

I. INTRODUCTION

Searching for the Higgs boson is the most important task for the Fermilab Tevatron collider and the CERN Large Hadron Collider (LHC). Among various Higgs production mechanisms, those induced by the bottom quark Yukawa coupling are particularly important because in some extensions of the Standard Model (SM) such a coupling could be considerably enhanced and thus the production rates can be much larger than the SM predictions. The Minimal Supersymmetric Standard Model (MSSM) [1] serve as a good example of such extensions, where the coupling of the lightest CP -even Higgs boson (denoted by h) to the bottom quark is proportional to $\tan\beta$ [2] and thus can be significantly enhanced by large $\tan\beta$.

In the production channels of the Higgs boson via its coupling to the bottom quark, the process $pp (p\bar{p}) \rightarrow bh + X$ via $bg \rightarrow bh$ was recently emphasized in Ref. [3]. The advantage of this process over the production via $b\bar{b} \rightarrow h$ [4], the dominant production channel via the bottom quark Yukawa coupling, is that the final bottom quark can be used to reduce backgrounds and to identify the Higgs boson production mechanism [5]. And compared with the production via $gg, q\bar{q} \rightarrow hbb$ [6], the production rate of $pp (p\bar{p}) \rightarrow bh + X$ is one order of magnitude larger. So the production $pp (p\bar{p}) \rightarrow bh + X$ may be a crucial channel for testing the bottom quark Yukawa coupling.

If the MSSM is indeed chosen by Nature, then the prediction of the cross section for the production $pp (p\bar{p}) \rightarrow bh + X$ [7] must be renewed with the inclusion of SUSY quantum corrections because, like the process of the charged Higgs boson production $pp (p\bar{p}) \rightarrow tH^- + X$ [8,9] and the relevant Higgs decays [10–12], the SUSY quantum corrections to this process may be quite large. In this work we study the one-loop SUSY-QCD corrections to this process, which is believed to be the dominant part in the SUSY corrections.

It is well known that the low-energy observables in the MSSM will recover their corresponding SM predictions when all sparticles as well as M_A (the mass of the CP-odd neutral Higgs boson) take their heavy limits. If only some of the masses take their heavy limits, e.g., all sparticles are heavy but M_A is light, then large remnant effects of SUSY may be left over in the physical observables of the Higgs sector. The study of these remnant effects will serve as an important probe for those heavy SUSY particles [11]. Such kind of study will be performed for the process $pp (p\bar{p}) \rightarrow bh + X$ in this work. After deriving the SUSY-QCD corrections to this process, we will examine the behavior of the corrections in the limit of heavy SUSY masses. When M_A is light and the sparticles take their heavy limits, we find the large remnant effects left over by the SUSY-QCD in such a Higgs production process.

This paper is organized as follows. In Section II we present our strategy for the calculation of the one-loop SUSY-QCD corrections to the process $pp (p\bar{p}) \rightarrow bh + X$. In Section III, we scan the parameter space of the MSSM to estimate the size of the SUSY-QCD corrections. In Section IV, we study the behaviors of these corrections in the limit of heavy SUSY masses. The conclusion is given in Section V and the detailed formula obtained in our calculations are presented in the Appendix.

II. CALCULATIONS

At high energy hadron colliders, the incoming b -quark is generated from gluons splitting into nearly collinear $b\bar{b}$ pairs. When one member of the pair initiates a hard-scattering subprocess, its partner tends to remain at low p_T and to become part of the beam remnant. Hence the final state typically has no high- p_T b -quarks. When the scale of the hard scattering is large compared with the b -quark mass, the b -quark is regarded as part of the proton sea [13]. However, unlike the light quark sea, the b -quark sea is perturbatively calculable. If the scale of the hard scattering is $\tilde{\mu}$ (for the scale we use $\tilde{\mu}$ to distinguish from the SUSY parameter μ), the b -quark distribution function $b(x, \tilde{\mu})$ is intrinsically of order $\alpha_s(\tilde{\mu}) \log(\tilde{\mu}/m_b)$. As $\tilde{\mu}$ approaches m_b from above, $b(x, \tilde{\mu}) \rightarrow 0$; while as $\tilde{\mu}$ becomes asymptotically large, $\alpha_s(\tilde{\mu}) \log(\tilde{\mu}/m_b)$ approaches order of unity and one needs to sum terms of order $\alpha_s^n(\tilde{\mu}) \log^n(\tilde{\mu}/m_b)$ into the b -quark distribution function to yield a well-behaved perturbation expansion in terms of α_s [13]. In this case, the b -quark distribution function becomes of the same order as the light partons. The main uncertainty of b -quark distribution function comes from that of gluon distribution function which is about 10% [14].

The subprocess $gb \rightarrow bh$ occurs through both s -channel and t -channel shown in Fig. 1(a, b). The spin- and color-averaged differential cross section at tree-level is given by

$$\frac{d\tilde{\sigma}^0}{dt} = -\frac{\alpha_s(\tilde{\mu})}{24} \left(\frac{gm_b(\tilde{\mu})}{2m_W} \right)^2 \left(\frac{\sin \alpha}{\cos \beta} \right)^2 \frac{1}{\hat{s}^2} \frac{m_h^4 + (\hat{s} + \hat{t} - m_h^2)^2}{\hat{s}\hat{t}}, \quad (2.1)$$

where \hat{s} and \hat{t} are the usual Mandelstam variables, $\alpha_s(\tilde{\mu})$ is the running strong coupling, and $m_b(\tilde{\mu})$ is the running bottom quark mass [4]. α represents the mixing angle between the two CP-even Higgs boson eigenstates and β is defined by $\tan \beta = v_2/v_1$ with $v_{1,2}$ denoting the vacuum expectation values of the two Higgs doublets [2]. In Eq.(2.1), we use the \overline{MS} running mass of the b -quark rather than the pole mass to take into account large QCD logarithm corrections to the vertex $h\bar{b}$ [15]. The SM prediction of the cross section is recovered when setting $|\sin \alpha/\cos \beta| = 1$ [3]. Throughout the calculations we neglect the b -quark mass except in the b -quark Yukawa couplings.

The one-loop Feynman diagrams of SUSY-QCD corrections are shown in Fig. 1(c-r). In our calculations we use dimensional regularization to control the ultraviolet divergences in the virtual loop corrections. For the renormalization of strong coupling constant g_s , we employ the \overline{MS} scheme [16]. As to the $h\bar{b}$ Yukawa coupling, at one loop level to $\mathcal{O}(\alpha_s)$ it is given by

$$\bar{g}_{h\bar{b}} = g_{h\bar{b}} + \delta g_{h\bar{b}}^{QCD} + \delta g_{h\bar{b}}^{SQCD}, \quad (2.2)$$

where $\bar{g}_{h\bar{b}}$ denotes the one-loop coupling, $g_{h\bar{b}}$ is tree-level coupling, $\delta g_{h\bar{b}}^{QCD}$ is the radiative correction from pure QCD [15], and $\delta g_{h\bar{b}}^{SQCD}$ is the one-loop SUSY-QCD contribution [11]. In determining $\delta g_{h\bar{b}}^{QCD} + \delta g_{h\bar{b}}^{SQCD}$, one needs the counter-term of the vertex $h\bar{b}\bar{b}$, whose general form is given by $g_{h\bar{b}}(\frac{\delta m_b^{QCD}}{m_b} + \frac{\delta m_b^{SQCD}}{m_b})$ with δm_b being the counter-term of the b -quark mass defined by $m_b^0 = m_b + \delta m_b$ (m_b^0 is the bare mass). δm_b is determined by requiring m_b to be the pole of the one-loop corrected b -quark propagator [15,11,17]. One major difference between $\delta g_{h\bar{b}}^{QCD}$ and $\delta g_{h\bar{b}}^{SQCD}$ is that the former contains large logarithms $\alpha_s \log \frac{\tilde{\mu}}{m_b}$ of $\mathcal{O}(1)$ and thus one needs to introduce \overline{MS} running mass $m_b(\tilde{\mu})$ to absorb leading logarithms $\alpha_s^n \log \left(\frac{\tilde{\mu}}{m_b} \right)^n$ [15]. An extensive discussion about this issue in the MSSM was provided in Ref. [17].

The one-loop SUSY-QCD contribution to the amplitude of $gb \rightarrow bh$ can be written as

$$\delta M = \frac{ig_s^3 T^a}{16\pi^2} \frac{gm_b}{2m_W} \frac{\sin \alpha}{\cos \beta} \bar{u}(p_2) (C_1 \gamma^\mu P_L + C_2 \gamma^\mu P_R + C_3 \gamma^\mu \not{k} P_L + C_4 \gamma^\mu \not{k} P_R + C_5 p_1^\mu P_L + C_6 p_1^\mu P_R + C_7 p_1^\mu \not{k} P_L + C_8 p_1^\mu \not{k} P_R + C_9 p_2^\mu P_L + C_{10} p_2^\mu P_R + C_{11} p_2^\mu \not{k} P_L + C_{12} p_2^\mu \not{k} P_R) u(p_1) \epsilon_\mu(k), \quad (2.3)$$

where $P_{L,R} \equiv (1 \mp \gamma_5)/2$, $T^a \equiv \lambda^a/2$ with λ^a being the Gell-Mann matrices, and k , p_1 and p_2 are the momentum of the incoming gluon, incoming b -quark and the outgoing b -quark, respectively. g_s and m_b should be understood as the running ones in Eq.(2.1). The coefficients C_i arise from the loops and are given explicitly in Appendix A. We have checked that all the ultraviolet divergences canceled as a result of renormalizability of the MSSM.

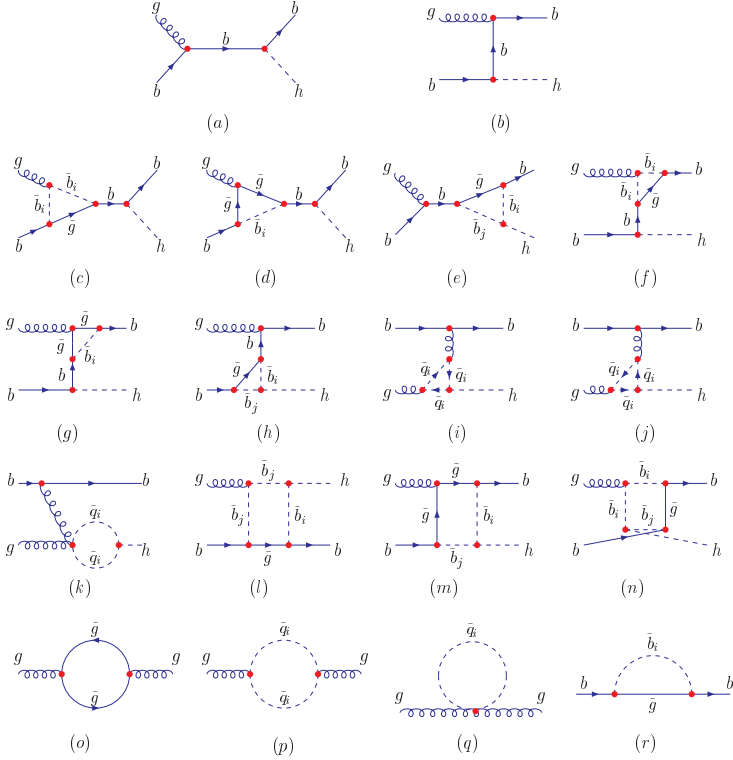


FIG. 1. Feynman diagrams of $gb \rightarrow bh$ with one-loop SUSY-QCD corrections: (a, b) are tree level diagrams; (c – e) are one-loop vertex diagrams for s -channel; (f – k) are one-loop vertex diagrams for t -channel ; (l – n) are the box diagrams; (o – r) are self-energy diagrams.

The differential cross section of $gb \rightarrow bh$ with one-loop SUSY-QCD corrections is given by

$$\frac{d\hat{\sigma}}{d\hat{t}} = \frac{d\hat{\sigma}^0}{d\hat{t}} + \frac{d(\Delta\hat{\sigma})}{d\hat{t}}, \quad (2.4)$$

where the first term is the tree-level result given in Eq.(2.1) and the second term is the one-loop SUSY-QCD corrections given by

$$\begin{aligned} \frac{d(\Delta\hat{\sigma})}{d\hat{t}} = & -\frac{\alpha_s \alpha_s}{48 4\pi} \left(\frac{\sin \alpha}{\cos \beta} \right)^2 \left(\frac{gm_b}{2m_W} \right)^2 \frac{1}{\hat{s}^2} \\ & \times \left[2(C_3 + C_4)m_h^2 + (C_5 + C_6) \frac{m_h^2(\hat{s} + \hat{t} - m_h^2)}{\hat{t}} + (C_9 + C_{10}) \frac{-(\hat{s} + \hat{t} - m_h^2)^2}{\hat{s}} \right]. \end{aligned} \quad (2.5)$$

The cross section of $gb \rightarrow bh$ is then given by

$$\hat{\sigma}(\hat{s}) = \int_{\hat{t}_{min}}^{\hat{t}_{max}} d\hat{t} \frac{d\hat{\sigma}}{d\hat{t}}, \quad (2.6)$$

where $\hat{t}_{max} = 0$ and $\hat{t}_{min} = -\hat{s} + m_h^2$ with m_h denoting the Higgs mass. In order to avoid collinear divergence in Eq.(2.6) and to enable the outgoing b -jet to be tagged by silicon vertex detector at the Tevatron and the LHC , we require the transverse momentum of the outgoing b -jet to be larger than 15 GeV and apply a rapidity cut $|\eta_b| < 2.5$ for the LHC and $|\eta_b| < 2.0$ for the Tevatron.

The total hadronic cross section for pp ($p\bar{p}$) $\rightarrow bh + X$ can be obtained by folding the subprocess cross section $\hat{\sigma}$ with the parton luminosity

$$\sigma(s) = \int_{\tau_0}^1 d\tau \frac{dL}{d\tau} \hat{\sigma}(\hat{s} = s\tau), \quad (2.7)$$

where $\tau_0 = m_h^2/s$ and s denotes the pp ($p\bar{p}$) squared center-of-mass energy. $dL/d\tau$ is the parton luminosity given by

$$\frac{dL}{d\tau} = \int_{\tau}^1 \frac{dx}{x} [f_g^p(x, Q) f_b^p(\tau/x, Q) + (g \leftrightarrow b)], \quad (2.8)$$

where f_b^p and f_g^p are the b -quark and gluon distribution functions in a proton, respectively. In our numerical calculations, we used the CTEQ5L parton distribution functions [18]. We did not distinguish the factorization scale Q and the renormalization scale $\tilde{\mu}$, and assumed $\tilde{\mu} = Q = m_h$. The scale dependence of our results will be briefly discussed in the proceeding section.

The process pp ($p\bar{p}$) $\rightarrow bh + X$ has been extensively studied [3] in the framework of the Standard Model. Its cross section is found to be at the order of 1 fb for the Tevatron and 100 fb for the LHC, and the next-leading-order (NLO) QCD correction can enhance the production rate by $50\% \sim 60\%$ for the Tevatron and $20\% \sim 40\%$ for the LHC [3], depending on the applied cuts and the Higgs boson mass. We will incorporate such QCD corrections in our calculations for the production rate σ/σ_{SM} .

III. NUMERICAL RESULTS

In this section we will perform a scan over the SUSY parameter space to show the possible size of the SUSY-QCD corrections. Before performing numerical calculations, we take a look at the relevant parameters involved. For the SM parameters, we took $m_W = 80.448$ GeV, $m_Z = 91.187$ GeV, $m_t = 174.3$ GeV, $\bar{m}_b(\bar{m}_b) = 4.2$ GeV [19], $\sin^2 \theta_W = 0.223$ and $\alpha_s(m_Z) = 0.118$. We used the one-loop QCD running $\alpha_s(\tilde{\mu})$ and $m_b(\tilde{\mu})$.

For the SUSY parameters, apart from gluino mass, the mass parameters of sbottoms are involved. The sbottom squared-mass matrix is [2]

$$M_b^2 = \begin{pmatrix} m_{\tilde{b}_L}^2 & m_b X_b \\ m_b X_b & m_{\tilde{b}_R}^2 \end{pmatrix}, \quad (3.1)$$

where

$$m_{\tilde{b}_L}^2 = m_{\tilde{Q}}^2 + m_b^2 + m_Z^2 (I_3^b - Q_b \sin^2 \theta_W) \cos(2\beta), \quad (3.2)$$

$$m_{\tilde{b}_R}^2 = m_{\tilde{D}}^2 + m_b^2 + m_Z^2 Q_b \sin^2 \theta_W \cos(2\beta), \quad (3.3)$$

$$X_b = A_b - \mu \tan \beta. \quad (3.4)$$

Here $m_{\tilde{Q}}^2$ and $m_{\tilde{D}}^2$ are soft-breaking mass terms for left-handed squark doublet \tilde{Q} and right-handed down squark \tilde{D} , respectively. A_b is the coefficient of the trilinear term $H_1 \tilde{Q} \tilde{D}$ in soft-breaking terms and μ the bilinear coupling of the two Higgs doublet in the superpotential. $I_3^b = -1/2$ and $Q_b = -1/3$ are the isospin and electric charge of the b -quark, respectively. This mass square matrix can be diagonalized by a unitary rotation

$$\begin{pmatrix} \tilde{b}_L \\ \tilde{b}_R \end{pmatrix} = \begin{pmatrix} \cos \theta_b & -\sin \theta_b \\ \sin \theta_b & \cos \theta_b \end{pmatrix} \begin{pmatrix} \tilde{b}_1 \\ \tilde{b}_2 \end{pmatrix}, \quad (3.5)$$

and consequently θ_b and the masses of physical sbottoms $\tilde{b}_{1,2}$ can be expressed as

$$\tan 2\theta_b = \frac{2m_b X_b}{(m_{\tilde{b}_L}^2 - m_{\tilde{b}_R}^2)}, \quad (3.6)$$

$$m_{\tilde{b}_1}^2 = m_{\tilde{b}_L}^2 \cos^2 \theta_b + 2m_b X_b \cos \theta_b \sin \theta_b + m_{\tilde{b}_R}^2 \sin^2 \theta_b, \quad (3.7)$$

$$m_{\tilde{b}_2}^2 = m_{\tilde{b}_L}^2 \sin^2 \theta_b - 2m_b X_b \cos \theta_b \sin \theta_b + m_{\tilde{b}_R}^2 \cos^2 \theta_b. \quad (3.8)$$

From Eqs.(2.1,2.5,2.6) we know that the cross section also depends on the Higgs mass, α and β , which can be determined at tree level by $\tan \beta$ and the CP-odd Higgs mass M_A [2]. Noticing the fact that both the mass and the mixing angle receive large radiative corrections when the SUSY scale is high above m_t [20], we used the loop-corrected relations of Higgs masses and mixing angle [21,22] in the computation of cross section. In our calculation, we used the program SUBHPOLE2 [21], where two-loop leading-log effects of the MSSM are incorporated in the Higgs masses and the mixing angel, to generate m_h and α needed for our computation. The input parameters for this program are the mass parameters in the top squark and sbottom sector, and M_A , $\tan \beta$ and the heavier chargino mass $m_{\tilde{\chi}}$.

We found that the usage of the loop-corrected relations of Higgs masses and mixing angle is indeed necessary. Comparing with the results obtained by using tree-level relations for Higgs masses and mixing angle, the size of SUSY-QCD corrections by using the loop-corrected relations is generally magnified from 30% to 200%¹. We also checked that this conclusion is also valid for the SUSY-QCD correction to the Higgs partial width $\Gamma(h \rightarrow b\bar{b})$.

Now we know the relevant parameters are

$$m_{\tilde{Q}}, m_{\tilde{U}}, m_{\tilde{D}}, A_{t,b}, m_{\tilde{g}}, m_{\tilde{\chi}}, \mu, M_A, \tan \beta, \quad (3.9)$$

where $M_{\tilde{U}}^2$ is the soft-breaking mass term for right-handed top-squark and A_t the coefficient of the soft-breaking trilinear term $H_2 \tilde{Q} \tilde{U}$. To show the main features of SUSY effects in pp ($p\bar{p}$) $\rightarrow bh + X$, we performed a scan over this ten-dimensional parameter space. In our scan we make no assumptions about the relations among these parameters to keep our result model-independent, but restrict the parameters with mass dimension to be less than 2 TeV. In addition, we consider the following experimental constraints:

- (1) $\mu > 0$ and $\tan \beta$ in the range $5 \leq \tan \beta \leq 50$, which seems to be favored by the muon $g - 2$ measurement [23].
- (2) The LEP and CDF lower mass bounds on Higgs, gluino, stop, sbottom and chargino [24,25]

$$m_h \geq 114 \text{ GeV}, m_{\tilde{t}_1} \geq 86.4 \text{ GeV}, m_{\tilde{b}_1} \geq 75.0 \text{ GeV}, m_{\tilde{g}} \geq 190 \text{ GeV}, m_{\tilde{\chi}}^{light} \geq 67.7 \text{ GeV}, \quad (3.10)$$

where $m_{\tilde{\chi}}^{light}$ is the mass of the lighter chargino.

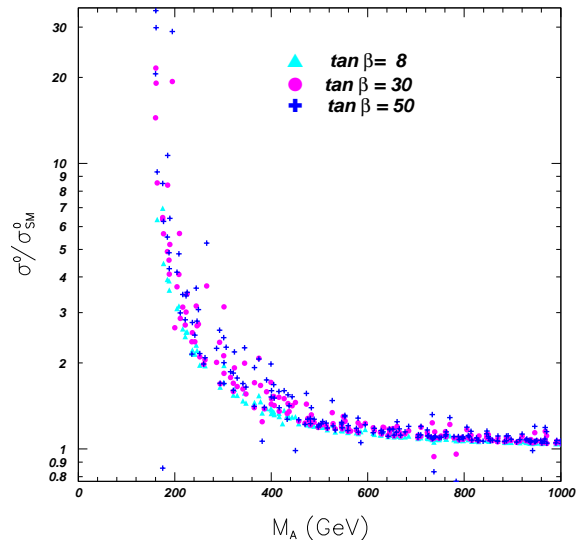


FIG. 2. The scatter plot of σ^0/σ_{SM}^0 versus M_A .

It would be interesting to first scan over the allowed parameter space to figure out how large the production rate is enhanced in the MSSM. In Fig.2 we present the tree-level cross section relative to the SM prediction with the same Higgs mass. This ratio is independent of collider energy, but is dependent on the SUSY mass parameters since we use the loop-corrected relations of the Higgs masses and the mixing angle (see the second paragraph of Sect. II). From Fig.2 one sees that the production rate in the MSSM can be significant larger than the SM prediction for a light M_A ; while for a heavy M_A the MSSM prediction approaches to the SM value. This character was first noticed in [26] and,

¹The main reason for such an enhancement is that for a large SUSY scale, the dominant term of the SUSY-QCD correction is proportional to $\cot \alpha + \tan \beta$ (see for example, Eqs.(4.2, 4.4, 4.6, 4.9) in the proceeding section), whose value obtained by using the loop-corrected relations of the Higgs masses and the mixing angle is generally larger than that by using the tree-level relations.

as a result of this character, distinguishing the lightest MSSM Higgs boson from the SM Higgs boson in the large M_A limit will be very difficult. When SUSY-QCD corrections are added, this character remains unchanged for heavy sbottoms (see following discussions). From Fig.2 one also finds that there exists the possibility (although very rare) that the MSSM cross section is suppressed to be below the SM value [27]. In this case, the SUSY-QCD corrections will play a more important role in Higgs phenomenology at colliders [28].

Now let us scan over the allowed parameter space to show the possible size of the SUSY-QCD corrections relative to the tree-level value. In our numerical evaluation, we found the relative correction is insensitive to collider energy. The difference of the results between the LHC and the Tevatron is at the level of parts per mill. In Fig.3 we present the SUSY-QCD corrections to the cross section.

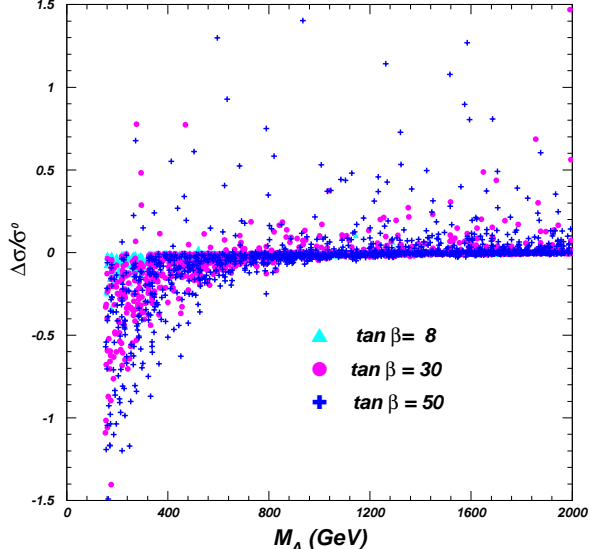


FIG. 3. The scatter plot of the SUSY-QCD correction $\Delta\sigma/\sigma^0$ versus M_A for the Tevatron. The difference of the results between the LHC and the Tevatron is at the level of parts per mill.

Fig.3 manifests three features of SUSY-QCD corrections for large $\tan\beta$. The first one is that the correction size is enhanced by $\tan\beta$ and thus can be quite large. The second one is that for M_A lighter than 500 GeV, the correction tends to be negative. The third one is that for large M_A , the correction may be positive and the maximum value seems to be independent of the value of M_A . These features can be explained as follows.

For the correction size larger than 2%, the dominant contribution of the SUSY-QCD correction is from the loop corrections to the vertex $h\bar{b}b$ and the contribution of the box diagrams is much smaller for the parameters satisfying the constraints in the paragraph following Eq.(3.9)². As a result, the correction behaves like (which is similar to the SUSY-QCD correction to the vertex $h\bar{b}b$ in case of heavy sbottoms [11])

$$\frac{\Delta\sigma}{\sigma^0} \sim C_1 \frac{M_{EW}^2}{M_A^2} + C_2 \frac{M_{EW}^2}{M_{\tilde{b}}^2}, \quad (3.11)$$

where M_{EW} and $M_{\tilde{b}}$ denote the electroweak scale and the typical mass of sbottoms, respectively. C_1 and C_2 are functions of $m_{\tilde{b}_1}$, $m_{\tilde{b}_2}$, $m_{\tilde{g}}$, μ and A_b , but independent of M_A . It is found that in general C_1 is negative and C_2 is positive and either C_1 or both C_1 and C_2 are enhanced by large $\tan\beta$. For a light M_A compared with $m_{\tilde{b}}$, the first term of the RHS in Eq.(3.11) is dominant and hence the cross section tends to be negative. While for a large M_A , the second term is dominant and the cross section tends to be positive. So the behavior of Eq.(3.11) can explain the features of Fig.3.

From Fig.3 we noticed that in some corners of parameter space the one-loop SUSY-QCD contributions to the cross section are comparable or even larger than the tree-level result and consequently, one must consider higher order corrections. In such cases, it is important to sum over the terms $\alpha_s^n \left(\frac{\mu}{M_{SUSY}}\right)^n$ to all orders of perturbation theory by using an effective Lagrangian approach [17,29].

²In the large limit of SUSY mass parameters discussed in the proceeding section, we have checked that, even for the correction size far smaller than 1%, the dominant contribution still comes from the corrections to the vertex $h\bar{b}b$.

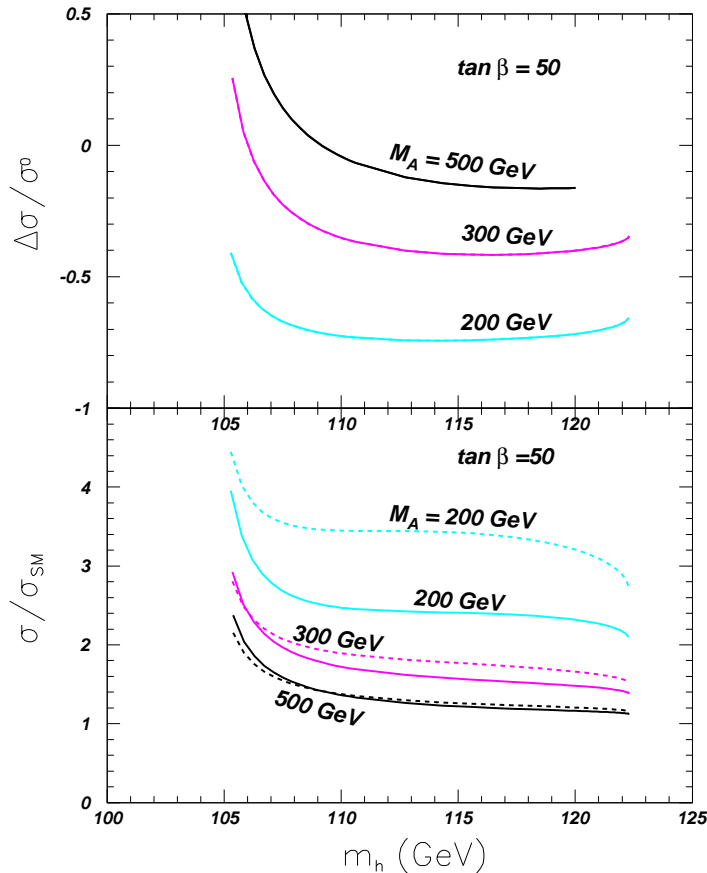


FIG. 4. The SUSY-QCD correction $\delta\sigma/\sigma^0$ and the cross section σ/σ_{SM} versus the mass of the produced Higgs boson. Solid curves are for the LHC and the dashed for the Tevatron. For $\Delta\sigma/\sigma^0$, each solid curve overlaps with the corresponding dashed one due to the tiny difference.

Next we study the dependence of the SUSY-QCD correction $\delta\sigma/\sigma^0$ and the cross section normalized by the SM prediction, σ/σ_{SM} , on the mass of the produced Higgs boson, which can be directly compared with experiment results and hence is much informative. In such a study we assumed a common value (M_{SUSY}) for all input SUSY mass parameters and, considering the fact that m_h is insensitive to M_A for $M_A > 150\text{GeV}$ [22], we fixed the value of M_A . Then through varying the value of M_{SUSY} , we obtain the different mass value of the Higgs boson.

The dependence on m_h is illustrated in Fig.4 for $\tan\beta = 50$. (Note that m_h can vary only in a small range since it is stringently upper bounded in the MSSM.) In this figure and also in the following figures showing σ/σ_{SM} , we also incorporated the conventional QCD corrections [3] into both the MSSM and the SM cross sections. As pointed out earlier, the SUSY-QCD correction $\delta\sigma/\sigma^0$ is not sensitive to collider energy. The difference of the results between the LHC and the Tevatron is too small to be visible, as shown in the upper part of Fig.4. But for σ/σ_{SM} the difference between the LHC and the Tevatron is visible since the QCD corrections are significantly different for these two colliders [3].

We also studied the dependence of the production rate on the renormalization scale $\tilde{\mu}$. (As pointed out earlier, we assume that the factorization scale is equal to the renormalization scale.) We found that such a scale dependence is significant in some parameter space. For example, for the LHC with $M_A = 300\text{ GeV}$ and $m_h = 120\text{ GeV}$, the ratio $\sigma(\tilde{\mu})/\sigma(m_h)$ is 0.93 for $\tilde{\mu} = m_h/2$ and 1.03 for $\tilde{\mu} = 2m_h$. Such an uncertainty is comparable with the uncertainty from the b -quark Yukawa coupling ($\bar{m}_b(\bar{m}_b) = 4.2 \pm 0.2$) and the parton distribution function (about 10%).

IV. BEHAVIOURS OF SUSY-QCD CORRECTIONS IN DECOUPLING LIMITS

To study the behaviors of the SUSY-QCD correction in the large limit of SUSY mass parameters, we consider four typical cases as in Ref. [11] where the decoupling property of SUSY-QCD correction to the coupling of $h\bar{b}b$ is

analyzed. To qualitatively understand the feature of each case, we present the approximate formula in the limits, but in practical numerical calculations we use the complete one-loop expressions.

About the inputs of the SUSY parameters, there are several differences between our work and Ref. [11]. The first one is that in [11] the tree-level relations for the Higgs masses and the mixing angle were used, but in our calculations we use the loop-corrected relations. As discussed earlier, using the loop-corrected relations leads to a significantly different correction. The second one is that in our analysis we considered the experimental bounds in Eq.(3.10). This will rule out some parameter space which have been considered in Ref. [11]. The third one is that in cases B and D we also require $A_{t,b}$ to be large since large $A_{t,b}$ is favored by the Higgs mass bound.

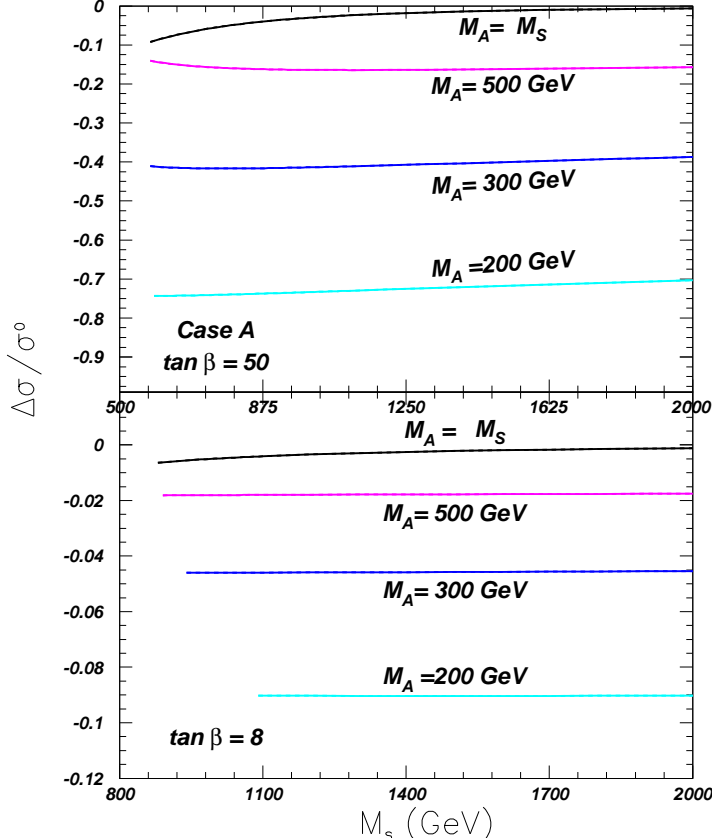


FIG. 5. The SUSY-QCD correction $\Delta\sigma/\sigma^0$ versus M_S in Case A. For each fixed value of M_A , the solid curve (for the LHC) overlaps with the corresponding dashed one (for the Tevatron) due to the tiny difference.

(1) *Case A*: All SUSY mass parameters except M_A are of the same size (collectively denoted by M_S) and tend to heavy, i.e.,

$$m_{\tilde{Q}} \sim m_{\tilde{U}} \sim m_{\tilde{D}} \sim A_b \sim A_t \sim m_{\tilde{g}} \sim \mu \sim M_S. \quad (4.1)$$

In this case the SUSY-QCD correction behaves like

$$\frac{\Delta\sigma}{\sigma^0} \sim \frac{2\alpha_s}{3\pi} \left[-(\tan\beta + \cot\alpha) - \cot\alpha \left(\frac{m_h^2}{12M_S^2} + \frac{m_b^2 \tan^2\beta}{2M_S^2} \right) + \frac{\tan\beta \cos\beta \sin(\alpha + \beta)}{3 \sin\alpha} \frac{m_Z^2}{M_S^2} \right], \quad (4.2)$$

where the first term in the RHS corresponds to the first term in Eq.(3.11)³ and the rest corresponds to the second term in Eq.(3.11). The striking feature of this case is that for very large M_S , the correction approaches a nonzero

³In the MSSM the tree-level relation for Higgs masses and mixing angle predicts the following relation: $\cot\alpha = -\tan\beta - \frac{2m_Z^2}{M_A^2} \tan\beta \cos 2\beta + O(\frac{m_Z^4}{M_A^4})$ and at loop level, the gap between $\cot\alpha$ and $-\tan\beta$ is generally enlarged.

constant, and this remnant effect of SUSY-QCD corrections is enhanced by large $\tan\beta$. This feature is illustrated in Fig.5. From Fig.5 one also finds that the SUSY-QCD correction in this case is negative and sizable⁴ for a light M_A and a large $\tan\beta$.

In Fig.6 we show the loop corrected cross section normalized by the SM prediction. From this figure we see that for M_A of several hundred GeV, although the tree-level cross section in the MSSM can be reduced by large SUSY-QCD corrections, an enhancement of several times over the SM prediction can still be expected due to the fact that the tree-level b -quark Yukawa coupling in the MSSM is significantly enhanced by large $\tan\beta$ for light M_A . This large enhancement shows a very weak dependence on M_S . So we can conclude that up to the next-leading order, a light M_A is still able to make the MSSM cross section larger than the SM prediction.

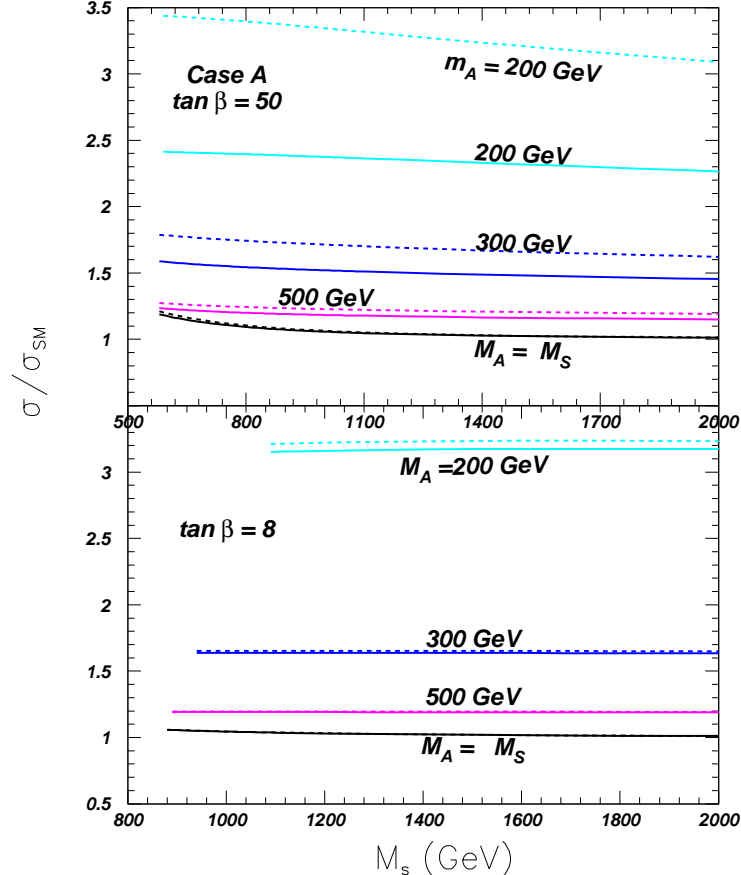


FIG. 6. σ/σ_{SM} versus M_A in Case A for the LHC (solid) and the Tevatron (dashed).

(2) *Case B*: $M_{\tilde{Q}}, M_{\tilde{U}}, M_{\tilde{D}}$ and $A_{t,b}$ (collectively denoted as M_S) is much larger than $\mu, m_{\tilde{g}}$ and M_A (collectively denoted as M), i.e.,

$$M_{\tilde{Q},\tilde{U},\tilde{D}} \sim A_{t,b} \sim M_S \gg m_{\tilde{g}} \sim \mu \sim M_A \sim M. \quad (4.3)$$

In this case the SUSY-QCD correction behaves as

$$\begin{aligned} \frac{\Delta\sigma}{\sigma^0} \sim & \frac{2\alpha_s}{3\pi} \left[\frac{-2M^2}{M_S^2} (\tan\beta + \cot\alpha) - \frac{m_h^2 M^2}{6M_S^4} \left(\frac{M_S}{M} + \cot\alpha \right) \right. \\ & \left. - \frac{m_Z^2}{2M_S^2} \frac{\cos\beta \sin(\alpha + \beta)}{\sin\alpha} \left(1 - \left(\frac{M_S}{M} - \tan\beta \right) \frac{2M^2}{M_S^2} \right) \right]. \end{aligned} \quad (4.4)$$

⁴If the correction is too sizable (say exceed 50%), higher order corrections are also important and need a proper treatment [17,29].

From this expression we see that in the large M_S limit, the SUSY-QCD corrections decouple rapidly as M^2/M_S^2 and the decoupling behavior is slowed down by large $\tan \beta$. The characters of this case are shown in Fig.7. So we see that even with a fixed light M_A , the process still does not have remnant SUSY-QCD effects if the gluino mass and μ are also kept light.

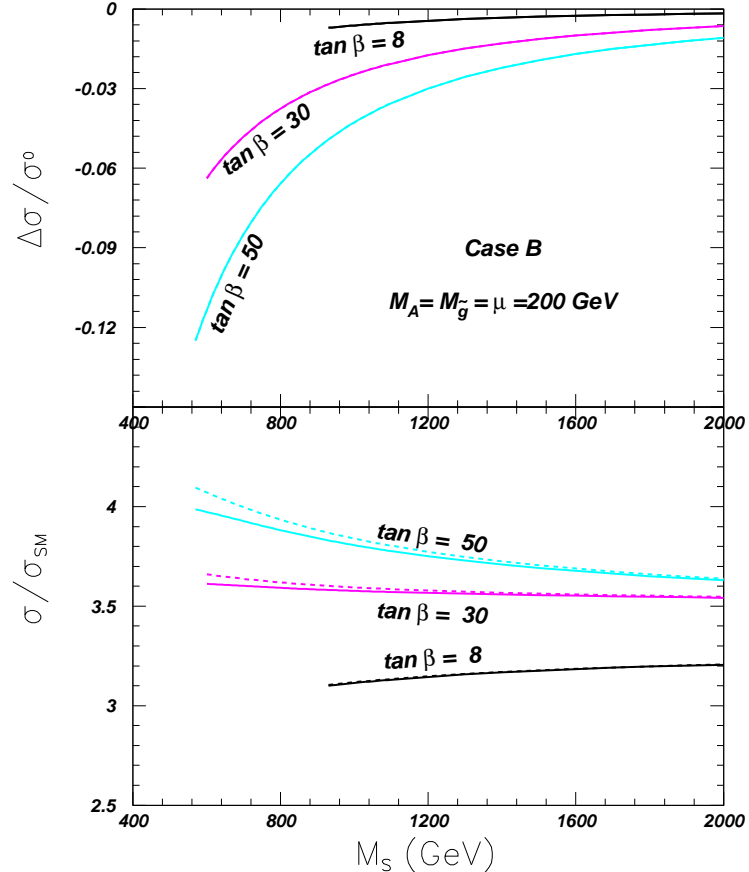


FIG. 7. The SUSY-QCD correction $\Delta\sigma/\sigma^0$ and σ/σ_{SM} versus M_S in Case B. The solid curves are for the LHC and the dashed for the Tevatron. For $\Delta\sigma/\sigma^0$, each solid curve overlaps with the corresponding dashed one due to the tiny difference.

(3) *Case C*: Only the gluino mass gets much larger than other SUSY parameters (collectively denoted as M_S) ⁵:

$$m_{\tilde{g}} \gg M_{\tilde{Q}, \tilde{U}, \tilde{D}} \sim A_{t,b} \sim \mu \sim M_A \sim M_S. \quad (4.5)$$

In this case the SUSY-QCD correction behaves as

$$\begin{aligned} \frac{\Delta\sigma}{\sigma^0} \simeq \frac{2\alpha_s}{3\pi} & \left[\frac{2M_S}{M_{\tilde{g}}} (\tan \beta + \cot \alpha) \left(1 - \log \frac{M_{\tilde{g}}^2}{M_S^2} \right) - \frac{M_S \cot \alpha}{3M_{\tilde{g}}} \frac{m_h^2}{M_S^2} \right. \\ & \left. + \frac{M_S \tan \beta}{M_{\tilde{g}}} \frac{m_Z^2}{M_S^2} \frac{\cos \beta \sin(\alpha + \beta)}{\sin \alpha} - \frac{m_b^2 \tan^2 \beta \cot \alpha}{M_{\tilde{g}} M_S} \right]. \end{aligned} \quad (4.6)$$

The main character of this case is that as gluino mass gets large, the correction drops very slowly like $\frac{1}{m_{\tilde{g}}} \log \frac{m_{\tilde{g}}^2}{M_S^2}$, which was also observed in Refs. [11,12]. Again, like other cases, the size of the correction is enhanced by large $\tan \beta$. In Fig.8 we show the dependence of the SUSY-QCD correction and σ/σ_{SM} on the gluino mass. Note that in this

⁵In this case the Higgs mass bound requires M_S to be much larger than electroweak scale.

case we found that $\tan \beta = 8$ cannot satisfy the experimental bounds in Eq.(3.10) for $M_S = 600$ GeV. In Fig.8 the correction size is significantly smaller than those in Case A and B. The reason is that here a large M_A is chosen so that $\tan \beta + \cos \alpha$ is suppressed (see footnote 3).

Let us explain the origin of the slowness of the decoupling in this case. Such slowness of the decoupling arises from the first term in Eq.(4.6), i.e., $\frac{2\mu}{M_{\tilde{q}}}(\tan \beta + \cot \alpha) \log \frac{M_{\tilde{q}}^2}{M_{\tilde{q}}^2}$ (note that the M_S in the factor $\frac{2M_S}{M_{\tilde{q}}}$ is μ and the one in the logarithm is squark mass $M_{\tilde{q}}$). As $M_{\tilde{q}}$ gets much larger than $M_{\tilde{q}}$ and μ , $\frac{2\mu}{M_{\tilde{q}}}$ decreases but $\log \frac{M_{\tilde{q}}^2}{M_{\tilde{q}}^2}$ increases. For the example shown in Fig.8, i.e., $M_{\tilde{q}}$ is changing from 1 TeV to 5 TeV with fixed $M_{\tilde{q}} = \mu = 600$ GeV, the factor $\frac{2\mu}{M_{\tilde{q}}}$ is decreased by 1/5 but the factor $\log \frac{M_{\tilde{q}}^2}{M_{\tilde{q}}^2}$ is increased by 4.16. Thus the slowness of the decoupling as gluino gets heavy is caused by the enlarged mass splitting between gluino and squark. Of course, since $\tan \beta + \cot \alpha$ is proportional to $\frac{2m_Z^2}{M_A^2} \tan \beta \cos 2\beta$ (see footnote 3), the contribution of the first term in Eq.(4.6) will be decoupled rapidly if M_A gets large.

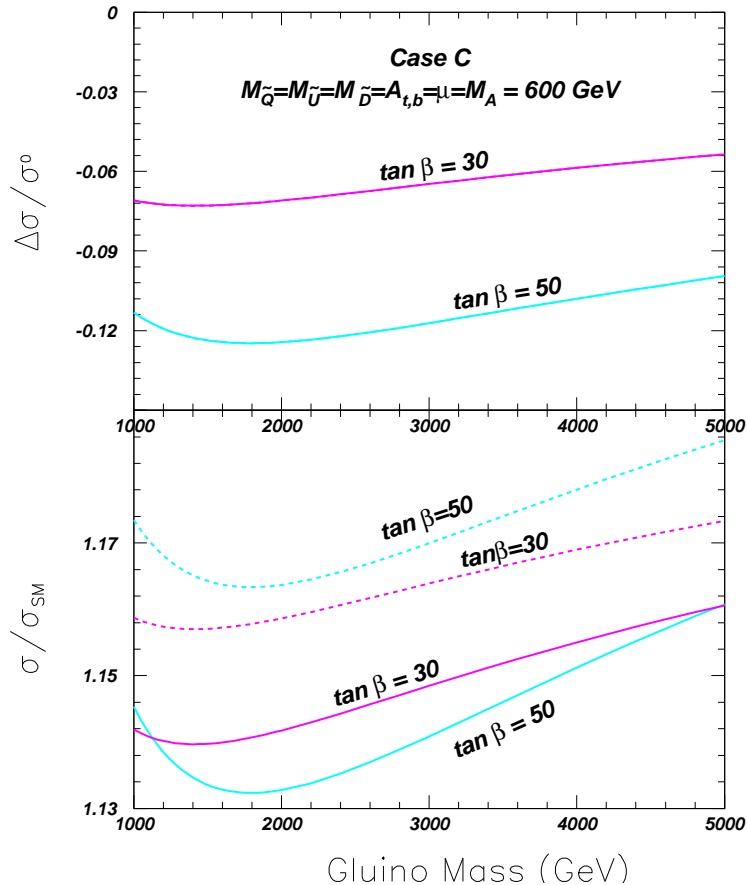


FIG. 8. The SUSY-QCD correction $\Delta\sigma/\sigma^0$ and σ/σ_{SM} versus the gluino mass in Case C. The solid curves are for the LHC and the dashed for the Tevatron. For $\Delta\sigma/\sigma^0$, each solid curve overlaps with the corresponding dashed one due to the tiny difference.

(4) *Case D*: One of the sbottoms and $A_{t,b}$ become heavy while other mass parameters (denoted as M) are fixed. We choose

$$M_{\tilde{D}} \sim M_{\tilde{U}} \sim A_{t,b} \gg M_{\tilde{Q}} \sim m_{\tilde{g}} \sim \mu \sim M_A \sim M \gg M_{EW} \quad (4.7)$$

or equally

$$m_{\tilde{b}_2} \sim m_{\tilde{t}_2} \sim A_{t,b} \gg m_{\tilde{b}_1} \sim m_{\tilde{t}_1} \sim m_{\tilde{g}} \sim \mu \sim M \gg M_{EW}, \quad (4.8)$$

where $m_{\tilde{b}_{1,2}}$ and $m_{\tilde{t}_{1,2}}$ are the masses of bottom-squarks and top-squarks, respectively.

In this case the SUSY-QCD correction behaves as

$$\frac{\Delta\sigma}{\sigma^0} \simeq \frac{2\alpha_s}{3\pi} \left[\frac{2M^2}{m_{\tilde{b}_2}^2} (\tan\beta + \cot\alpha) \left(1 + \log \frac{M^2}{m_{\tilde{b}_2}^2} \right) + \frac{m_Z^2}{m_{\tilde{b}_2}^2} \frac{\cos\beta \sin(\alpha + \beta)}{\sin\alpha} \left(-1 + \frac{2}{3} s_W^2 \right) \left(\frac{m_{\tilde{b}_2}}{m_{\tilde{b}_1}} - \tan\beta \right) \right]. \quad (4.9)$$

The main feature of this case is the correction decouples like $\frac{1}{m_{\tilde{b}_2}^2} \log \frac{M^2}{m_{\tilde{b}_2}^2}$ and this decoupling behavior is slowed down by large $\tan\beta$. Fig.9 shows the dependence of the correction and the cross section on $m_{\tilde{D}}$ ($\sim m_{\tilde{b}_2}$). Comparing with the results in case B, we see that the correction size decrease more slowly as $m_{\tilde{D}}$ gets heavy.

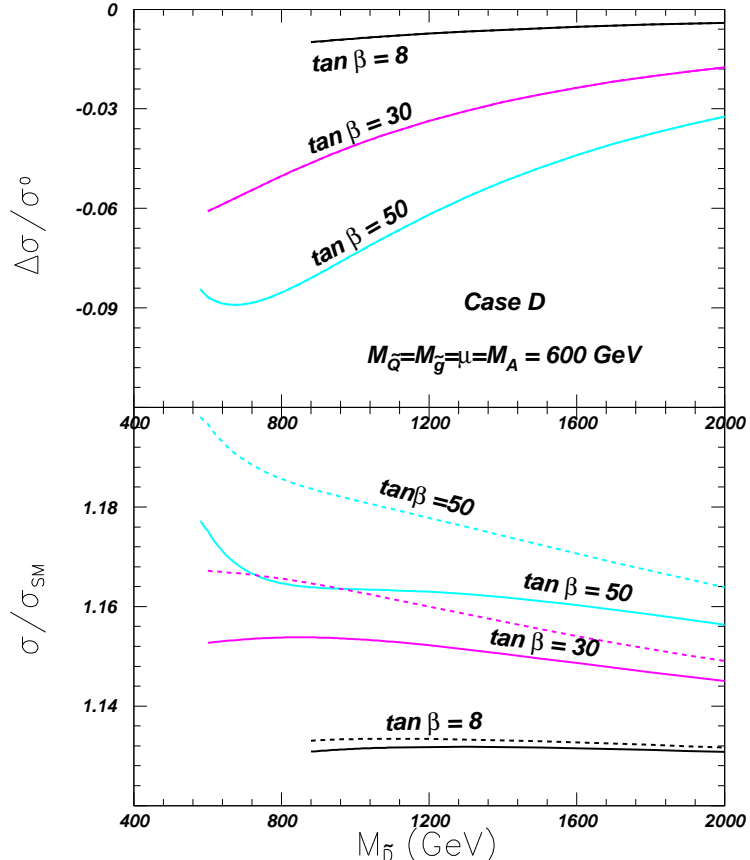


FIG. 9. The SUSY-QCD correction $\Delta\sigma/\sigma^0$ and σ/σ_{SM} versus $M_{\tilde{D}}$ in Case D for the LHC (solid curves) and the Tevatron (dashed curves). For $\Delta\sigma/\sigma^0$, each solid curve overlaps with the corresponding dashed one due to the tiny difference.

From the above analyses we see that when M_A is fixed and all other SUSY mass parameters get large, the SUSY-QCD lefts over some remnant effects in the Higgs production process $pp \rightarrow bh + X$ at the hadron colliders. Note that for the remnant effects to be left over, μ and gluino mass must be comparable with or larger than the masses of the sbottoms. The fundamental reason for such a behavior is that the couplings like $h\tilde{b}_i\tilde{b}_j$ are proportional to SUSY mass parameters.

We conclude this section by making a few remarks. Firstly, in our analysis we assumed $m_{\tilde{g}}, \mu > 0$ and, as a result, all four cases have negative values of the correction. In the anomaly-mediated SUSY breaking scenario [30], a negative $m_{\tilde{g}}$ is predicted and in this case, the sign of the correction may be reversed. Secondly, it should be noted that in the calculations of such Higgs processes it is necessary to use the loop-corrected relations of the Higgs masses and the mixing angle since such relations can significantly affect the results. Thirdly, in case of a light M_A , although the SUSY-QCD corrections tend to reduce the cross section severely, the MSSM cross section can still be several times larger than the SM prediction. If the cross section of this process is measured in the future and found to be several times larger than the SM prediction, a light M_A is favored.

V. CONCLUSION

In this work, we studied the one-loop SUSY-QCD quantum effects in the Higgs production $pp (p\bar{p}) \rightarrow bh + X$ at the Tevatron and the LHC in the framework of the MSSM. We found that for a light M_A and large $\tan\beta$, the corrections can be quite sizable and cannot be neglected. We performed a detailed analysis on the behaviors of the corrections in the limits of heavy SUSY masses and found that when M_A is fixed and all other SUSY mass parameters get large, the SUSY-QCD lefts over some remnant effects in the Higgs production process $pp \rightarrow bh + X$. Such remnant effects can be so sizable for a light M_A that they might be observable in the future experiment. The exploration of such remnant effects is important for probing SUSY, especially in case that the sparticles are too heavy (above TeV) to be directly discovered in future experiments.

ACKNOWLEDGMENT

We thank Tao Han for discussions. This work is supported in part by the Chinese Natural Science Foundation and by the US Department of Energy, Division of High Energy Physics under grant No. DE-FG02-91-ER4086.

APPENDIX A: EXPRESSIONS OF FORM FACTORS

Before presenting the explicit form of C_i s, we define the following abbreviations:

$$\hat{s} = (p_1 + k)^2, \quad \hat{t} = (k - p_2)^2, \quad (A1)$$

$$a_{1,2} = \frac{1}{\sqrt{2}}(\sin\theta_b \mp \cos\theta_b), \quad b_{1,2} = \frac{1}{\sqrt{2}}(\cos\theta_b \pm \sin\theta_b), \quad (A2)$$

$$A_I^L = (a_I - b_I)^2, \quad A_I^R = (a_I + b_I)^2, \quad A_I = a_I^2 - b_I^2, \quad (I = 1, 2), \quad (A3)$$

$$A_{IJ}^L = a_I a_J + b_I b_J + a_I b_J + b_I a_J, \quad A_{IJ}^R = a_I a_J + b_I b_J - a_I b_J - b_I a_J, \quad (A4)$$

$$B_{IJ}^L = a_I a_J - b_I b_J - a_I b_J + b_I a_J, \quad B_{IJ}^R = a_I a_J - b_I b_J + a_I b_J - b_I a_J, \quad (A5)$$

$$cc_1 = -\frac{m_Z}{\cos\theta_W} \left(\frac{1}{2} - \frac{1}{3} \sin^2\theta_W \right) \sin(\alpha + \beta), \quad (A6)$$

$$cc_2 = -\frac{m_Z}{\cos\theta_W} \frac{1}{3} \sin^2\theta_W \sin(\alpha + \beta), \quad cc_3 = \frac{m_b}{2m_W \cos\beta} (A_b \sin\alpha + \mu \cos\alpha), \quad (A7)$$

$$Q_{11} = cc_1 \cos^2\theta_b + cc_2 \sin^2\theta_b + 2cc_3 \sin\theta_b \cos\theta_b, \quad (A8)$$

$$Q_{12} = (cc_2 - cc_1) \sin\theta_b \cos\theta_b + cc_3(\cos^2\theta_b - \sin^2\theta_b), \quad (A9)$$

$$Q_{21} = (cc_2 - cc_1) \sin\theta_b \cos\theta_b + cc_3(\cos^2\theta_b - \sin^2\theta_b), \quad (A10)$$

$$Q_{22} = cc_1 \sin^2\theta_b + cc_2 \cos^2\theta_b - 2cc_3 \sin\theta_b \cos\theta_b, \quad (A11)$$

$$B_i^I = B_i(p, m_{\tilde{g}}, m_{\tilde{b}_I})|_{p^2=m_b^2}, \quad (A12)$$

$$B_i^s{}^I = B_i(p, m_{\tilde{g}}, m_{\tilde{b}_I})|_{p^2=\hat{s}}, \quad B_i^t{}^I = B_i(p, m_{\tilde{g}}, m_{\tilde{b}_I})|_{p^2=\hat{t}}, \quad (A13)$$

$$C_{ij}^a{}^I = C_{ij}(p_1, k, m_{\tilde{b}_I}, m_{\tilde{g}}, m_g), \quad C_{ij}^b{}^I = C_{ij}(-p_1, -k, m_{\tilde{g}}, m_{\tilde{b}_I}, m_{\tilde{b}_I}), \quad (A14)$$

$$C_{ij}^c{}^I = C_{ij}(-p_2, k, m_{\tilde{b}_I}, m_{\tilde{g}}, m_{\tilde{g}}), \quad C_{ij}^d{}^I = C_{ij}(-p_2, k, m_{\tilde{g}}, m_{\tilde{b}_I}, m_{\tilde{b}_I}), \quad (A15)$$

$$C_{ij}^e{}^{IJ} = C_{ij}(-p_2, -p_h, m_{\tilde{g}}, m_{\tilde{b}_I}, m_{\tilde{b}_J}), \quad C_{ij}^f{}^{IJ} = C_{ij}(-p_1, p_h, m_{\tilde{g}}, m_{\tilde{b}_J}, m_{\tilde{b}_I}), \quad (A16)$$

$$D_{ij}^g{}^{IJ} = D_{ij}(-p_1, -k, p_h, m_{\tilde{g}}, m_{\tilde{b}_J}, m_{\tilde{b}_I}, m_{\tilde{b}_I}), \quad D_{ij}^h{}^{IJ} = D_{ij}(-p_1, p_h, p_2, m_{\tilde{g}}, m_{\tilde{b}_J}, m_{\tilde{b}_I}, m_{\tilde{g}}), \quad (A17)$$

$$D_{ij}^k{}^{IJ} = D_{ij}(-p_2, k, -p_h, m_{\tilde{g}}, m_{\tilde{b}_I}, m_{\tilde{b}_I}, m_{\tilde{b}_J}), \quad (A18)$$

where B_i , C_{ij} and D_{ij} are loop functions defined in [31].

After $\frac{g_s^2}{16\pi^2}$ is factored out, the renormalization constant of b-quark can be expressed as

$$\delta Z_L = C_F \sum_{I=1}^2 A_I^L B_1^I, \quad \delta Z_R = C_F \sum_{I=1}^2 A_I^R B_1^I, \quad (A19)$$

$$\frac{\delta m_b}{m_b} = C_F \sum_{I=1}^2 \left(\frac{m_{\bar{g}}}{m_b} A_I B_0^I - \frac{1}{2} A_I^L B_1^I - \frac{1}{2} A_I^R B_1^I \right), \quad (\text{A20})$$

where $C_F = 4/3$. The contributions of the self-energy diagrams of b -quark propagator can be written as

$$\Sigma_L^s = C_F \sum_{I=1}^2 A_I^L B_1^s{}^I - \delta Z_L, \quad \Sigma_L^t = C_F \sum_{I=1}^2 A_I^L B_1^t{}^I - \delta Z_L, \quad (\text{A21})$$

$$\Sigma_R^s = C_F \sum_{I=1}^2 A_I^R B_1^s{}^I - \delta Z_R, \quad \Sigma_R^t = C_F \sum_{I=1}^2 A_I^R B_1^t{}^I - \delta Z_R. \quad (\text{A22})$$

C_i appeared in Eq.(2.5) are given by

$$\begin{aligned} C_3 = & \sum_{I=1}^2 \left\{ -\frac{3}{2} (\hat{s} C_{12}^a{}^I + \hat{s} C_{23}^a{}^I + 2 C_{24}^a{}^I - 1/2 - m_{\bar{g}}^2 C_0^a{}^I) A_I^L / \hat{s} + \frac{1}{3} C_{24}^b{}^I A_I^L / \hat{s} \right. \\ & - \frac{3}{2} (\hat{t} C_{12}^c{}^I + \hat{t} C_{23}^c{}^I + 2 C_{24}^c{}^I - 1/2 - m_{\bar{g}}^2 C_0^c{}^I) A_I^R / \hat{t} + \frac{1}{3} C_{24}^d{}^I A_I^R / \hat{t} \} \\ & - \delta Z_L / \hat{s} - \delta Z_R / \hat{t} - \Sigma_L^s / \hat{s} - \Sigma_R^t / \hat{t} - \left(\frac{1}{2} \delta Z_L + \frac{1}{2} \delta Z_R + \frac{\delta m_b}{m_b} \right) \left(\frac{1}{\hat{s}} + \frac{1}{\hat{t}} \right) \\ & \left. + \frac{2 m_W \cos \beta}{m_b \sin \alpha} \sum_{I,J=1}^2 Q_{IJ} \left\{ \frac{4}{3} m_{\bar{g}} C_0^e{}^{IJ} B_{IJ}^L / \hat{s} + \frac{4}{3} m_{\bar{g}} C_0^f{}^{IJ} B_{IJ}^L / \hat{t} + \frac{3}{2} m_{\bar{g}} D_0^h{}^{IJ} B_{IJ}^L \right\} \right\}, \end{aligned} \quad (\text{A23})$$

$$\begin{aligned} C_4 = & \sum_{I=1}^2 \left\{ -\frac{3}{2} (\hat{s} C_{12}^a{}^I + \hat{s} C_{23}^a{}^I + 2 C_{24}^a{}^I - 1/2 - m_{\bar{g}}^2 C_0^a{}^I) A_I^R / \hat{s} + \frac{1}{3} C_{24}^b{}^I A_I^R / \hat{s} \right. \\ & - \frac{3}{2} (\hat{t} C_{12}^c{}^I + \hat{t} C_{23}^c{}^I + 2 C_{24}^c{}^I - 1/2 - m_{\bar{g}}^2 C_0^c{}^I) A_I^L / \hat{t} + \frac{1}{3} C_{24}^d{}^I A_I^L / \hat{t} \} \\ & - \delta Z_R / \hat{s} - \delta Z_L / \hat{t} - \Sigma_R^s / \hat{s} - \Sigma_L^t / \hat{t} - \left(\frac{1}{2} \delta Z_L + \frac{1}{2} \delta Z_R + \frac{\delta m_b}{m_b} \right) \left(\frac{1}{\hat{s}} + \frac{1}{\hat{t}} \right) \\ & \left. + \frac{2 m_W \cos \beta}{m_b \sin \alpha} \sum_{I,J=1}^2 Q_{IJ} \left\{ \frac{4}{3} m_{\bar{g}} C_0^e{}^{IJ} B_{IJ}^R / \hat{s} + \frac{4}{3} m_{\bar{g}} C_0^f{}^{IJ} B_{IJ}^R / \hat{t} + \frac{3}{2} m_{\bar{g}} D_0^h{}^{IJ} B_{IJ}^R \right\} \right\}, \end{aligned} \quad (\text{A24})$$

$$\begin{aligned} C_5 = & \sum_{I=1}^2 \left\{ -\frac{3}{2} (-4 C_{24}^a{}^I + 1 + 2 m_{\bar{g}}^2 C_0^a{}^I) A_I^L / \hat{s} - \frac{1}{3} (\hat{s} C_{12}^b{}^I + \hat{s} C_{23}^b{}^I + 2 C_{24}^b{}^I) A_I^L / \hat{s} \right\} \\ & + 2 \delta Z_L / \hat{s} + 2 \Sigma_L^s / \hat{s} + (\delta Z_L + \delta Z_R + 2 \frac{\delta m_b}{m_b}) / \hat{s} + \frac{2 m_W \cos \beta}{m_b \sin \alpha} \sum_{I,J=1}^2 Q_{IJ} \left\{ -\frac{8}{3} m_{\bar{g}} C_0^e{}^{IJ} B_{IJ}^L / \hat{s} \right. \\ & \left. + \frac{1}{3} m_{\bar{g}} (D_0^g{}^{IJ} + D_{11}^g{}^{IJ} - D_{13}^g{}^{IJ}) B_{IJ}^L + 3 m_{\bar{g}} (D_{11}^h{}^{IJ} - D_{12}^h{}^{IJ}) B_{IJ}^L + \frac{1}{3} m_{\bar{g}} D_{13}^k B_{IJ}^L \right\}, \end{aligned} \quad (\text{A25})$$

$$\begin{aligned} C_6 = & \sum_{I=1}^2 \left\{ -\frac{3}{2} (-4 C_{24}^a{}^I + 1 + 2 m_{\bar{g}}^2 C_0^a{}^I) A_I^R / \hat{s} - \frac{1}{3} (\hat{s} C_{12}^b{}^I + \hat{s} C_{23}^b{}^I + 2 C_{24}^b{}^I) A_I^R / \hat{s} \right\} \\ & + 2 \delta Z_R / \hat{s} + 2 \Sigma_R^s / \hat{s} + (\delta Z_L + \delta Z_R + 2 \frac{\delta m_b}{m_b}) / \hat{s} + \frac{2 m_W \cos \beta}{m_b \sin \alpha} \sum_{I,J=1}^2 Q_{IJ} \left\{ -\frac{8}{3} m_{\bar{g}} C_0^e{}^{IJ} B_{IJ}^R / \hat{s} \right. \\ & \left. + \frac{1}{3} m_{\bar{g}} (D_0^g{}^{IJ} + D_{11}^g{}^{IJ} - D_{13}^g{}^{IJ}) B_{IJ}^R + 3 m_{\bar{g}} (D_{11}^h{}^{IJ} - D_{12}^h{}^{IJ}) B_{IJ}^R + \frac{1}{3} m_{\bar{g}} D_{13}^k B_{IJ}^R \right\}, \end{aligned} \quad (\text{A26})$$

$$\begin{aligned} C_9 = & \sum_{I=1}^2 \left\{ -\frac{3}{2} (-4 C_{24}^c{}^I + 1 + 2 m_{\bar{g}}^2 C_0^c{}^I) A_I^R / \hat{t} - \frac{1}{3} (\hat{t} C_{12}^d{}^I + \hat{t} C_{23}^d{}^I + 2 C_{24}^d{}^I) A_I^R / \hat{t} \right\} \\ & + 2 \delta Z_R / \hat{t} + 2 \Sigma_R^t / \hat{t} + (\delta Z_L + \delta Z_R + 2 \frac{\delta m_b}{m_b}) / \hat{t} + \frac{2 m_W \cos \beta}{m_b \sin \alpha} \sum_{I,J=1}^2 Q_{IJ} \left\{ -\frac{8}{3} m_{\bar{g}} C_0^f{}^{IJ} B_{IJ}^L / \hat{t} \right. \\ & \left. + \frac{1}{3} m_{\bar{g}} (D_0^g{}^{IJ} + D_{11}^g{}^{IJ} - D_{13}^g{}^{IJ}) B_{IJ}^L + 3 m_{\bar{g}} (D_{11}^h{}^{IJ} - D_{12}^h{}^{IJ}) B_{IJ}^L + \frac{1}{3} m_{\bar{g}} D_{13}^k B_{IJ}^L \right\} \end{aligned}$$

$$+ \frac{1}{3} m_{\tilde{g}} D_{13}^{g \, IJ} B_{IJ}^L + 3 m_{\tilde{g}} (D_{12}^{h \, IJ} - D_{13}^{h \, IJ}) B_{IJ}^L + \frac{1}{3} m_{\tilde{g}} (D_0^k + D_{11}^k - D_{13}^k) B_{ij}^L \}, \quad (\text{A27})$$

$$C_{10} = \sum_{I=1}^2 \left\{ -\frac{3}{2} (-4 C_{24}^c \, I + 1 + 2 m_{\tilde{g}}^2 C_0^c \, I) A_I^L / \hat{t} - \frac{1}{3} (\hat{t} C_{12}^{d \, I} + \hat{t} C_{23}^{d \, I} + 2 C_{24}^{d \, I}) A_I^L / \hat{t} \right\} \\ + 2 \delta Z_L / \hat{t} + 2 \Sigma_L^t / \hat{t} + (\delta Z_L + \delta Z_R + 2 \frac{\delta m_b}{m_b}) / \hat{t} + \frac{2 m_W \cos \beta}{m_b \sin \alpha} \sum_{I,J=1}^2 Q_{IJ} \left\{ -\frac{8}{3} m_{\tilde{g}} C_0^f \, IJ B_{IJ}^R / \hat{t} \right. \\ \left. + \frac{1}{3} m_{\tilde{g}} D_{13}^{g \, IJ} B_{IJ}^R + 3 m_{\tilde{g}} (D_{12}^{h \, IJ} - D_{13}^{h \, IJ}) B_{IJ}^R + \frac{1}{3} m_{\tilde{g}} (D_0^k + D_{11}^k - D_{13}^k) B_{ij}^R \right\}. \quad (\text{A28})$$

Since we have neglect the b-quark mass throughout this paper, $C_{1,2,7,8,11,12}$ are irrelevant to our result and we do not present their explicit forms here.

- [1] For a review, see, e.g., H. E. Haber, G. L. Kane, *Phys. Rept.* **117**, 75 (1985).
- [2] For a review, see, e.g., J. F. Gunion, H. E. Haber, G. L. Kane and S. Dawson, *The Higgs Hunter's Guide*, (Addison-Wesley, Reading, MA, 1990).
- [3] J. Campbell, R. K. Ellis, F. Maltoni and S. Willenbrock, hep-ph/0204093.
- [4] D. A. Dicus and S. Willenbrock, *Phys. Rev. D* **39**, 751 (1989); D. Dicus, T. Stelzer, Z. Sullivan and S. Willenbrock, *Phys. Rev. D* **59**, 094016 (1999).
- [5] M. Drees, M. Guchait and P. Roy, *Phys. Rev. Lett.* **80**, 2047(1998); Erratum-*ibid.* **81**, 2394(1998); M. Carena, S. Mrenna and C. E. Wagner, *Phys. Rev. D* **60**, 075010 (1999); ATLAS Collaboration, Technical Design Report, CERN-LHCC-99-15.
- [6] E. Richter-Was and D. Froidevaux, *Z. Phys. C* **76**, 665(1997); J. L. Diaz-Cruz, H. J. He, T. Tait and C. P. Yuan, *Phys. Rev. Lett.* **80**, 4641 (1998); C. Balazs, J. L. Diaz-Cruz, H. J. He, T. Tait and C. P. Yuan, *Phys. Rev. D* **59**, 055016 (1999); M. Carena *et al.*, Report of the Tevatron Higgs Working Group, hep-ph/0010338.
- [7] C.-S. Huang and S.-H. Zhu, *Phys. Rev. D* **60**, 075012(1999).
- [8] A. Belyaev, D. Garcia, J. Gausch and J. Sola, *Phys. Rev. D* **65**, 031701 (2002).
- [9] G. Gao, G. Lu, Z. Xiong and J. M. Yang, *Phys. Rev. D* **66**, 015007(2002).
- [10] C. S. Li and J. M. Yang, *Phys. Lett. B* **315**, 367 (1993); C. S. Li, B. Q. Hu and J. M. Yang, *D* **47**, 2865 (1993). J. M. Yang, C. S. Li and B. Q. Hu, *D* **47**, 2872 (1993); J. A. Coarasa, D. Garcia, J. Guasch, R. A. Jimenez, J. Sola, *Eur. Phys. J. C* **2**, 373 (1998); A. Dobado, M. J. Herrero, *Phys. Rev. D* **65**, 075023(2002); M. J. Herrero, S. Peñaranda and D. Temes, *Phys. Rev. D* **64**, 115003 (2001);
- [11] H. E. Haber, *et al.*, *Phys. Rev. D* **63**, 055004 (2001).
- [12] A. Dabelstein, *Nucl. Phys. B* **456**, 25(1995); S. Heinemeyer, W. Hollik and G. Weiglein, *Eur. Phys. J. C* **16**, 139(2000).
- [13] R. M. Barnett, H. E. Haber and D. E. Soper, *Nucl. Phys. B* **306**, 697 (1988); F. I. Olness and W. K. Tung, *Nucl. Phys. B* **308**, 813 (1988); M. A. Aivazis, J. C. Collins, F. I. Olness and W. K. Tung, *Phys. Rev. D* **50**, 3102 (1994); J. C. Collins, *Phys. Rev. D* **58**, 094002 (1998).
- [14] J. Huston, *et. al* *Phys. Rev. D* **58**, 114034(1998).
- [15] See, for example, E. Braaten and J. P. Leveille, *Phys. Rev. D* **22**, 715 (1980); M. Drees and K. Hikasa, *Phys. Lett. B* **240**, 455 (1990).
- [16] W. Beenakker, R. H'opker, and P. M. Zerwas, *Phys. Lett. B* **378**, 159 (1996); W. Beenakker, *et. al* *Z. Phys. C* **75**, 349 (1997).
- [17] M. Carena, D. Garcia, U. Nierste and C. E. M. Wagner, *Nucl. Phys. B* **577**, 88(2000).
- [18] H. L. Lai, *et al.* (CTEQ collaboration), hep-ph/9903282.
- [19] D. E. Groom *et al* [Partical Data Group Collaboration], *Eur. Phys. J. C* **15**, 1 (2000).
- [20] H. Haber and R. Hempfling, *Phys. Rev. Lett.* **66**, 1815(1991); M. Carena, J. R. Espinosa, M. Quiros and C. E. M. Wagner, *Phys. Lett. B* **355**, 209 (1995); H. Haber, R. Hempfling and A. H. Hoang, *Z. Phys. C* **57**, 539 (1997).
- [21] M. Carena, M. Quiros and C. E. M. Wagner, *Nucl. Phys. B* **461**, 407(1996); M. Carena, *et. al.*, *Nucl. Phys. B* **580**, 29(2000).
- [22] A. Dabelstein, *Z. Phys. C* **67**, 495(1995); S. Heinemeyer, W. Hollik and G. Weiglein, *Eur. Phys. J. C* **9**, 343(1999); J. R. Espinosa and R. J. Zhang, *Nucl. Phys. B* **586**, 3(2000); J. R. Espinosa, I. Navarro, *Nucl. Phys. B* **615**, 82(2001); G. Degrassi, P. Slavich, F. Zwirner, *Nucl. Phys. B* **611**, 403(2001); A. Brignole, G. Degrassi, P. Slavich, F. Zwirner, *Nucl. Phys. B* **631**, 195 (2002).
- [23] H. N Brown, *et al.*, Mu g-2 Collaboration, *Phys. Rev. Lett.* **86**, 2227 (2001).

- [24] R. Barate *et al.* [ALEPH Collaboration], Phys. Lett. B**499**, 53(2001); LEP Higgs Working Group, hep-ex/0107029 (LHWG/2001-03).
- [25] Particle Physics Group. Eur. Phys. J. C, **15**, 274 (2000).
- [26] H. E. Haber and Y. Nir, Nucl. Phys. B**335**, 363(1990).
- [27] G. L. Kane, G. D. Kribs, S. P. Martin and J. D. Wells, Phys. Rev. D**53**, 213 (1996); W. Loinaz and J. D. Wells, Phys. Lett. B**445**, 178 (1998); K. S. Babu and C. Kolda, Phys. Lett. B**451**, 77 (1999).
- [28] M. Carena, S. Mrenna and C. E. M. Wagner, Phys. Rev. D**62**, 055008(2000);
- [29] H. Eberl, et al., Phys. Rev. D **62**, 055006 (2000).
- [30] L. Randall and R. Sundrum, Nucl. Phys. B**557**, 79(1999); G. D. Kribs, Phys. Rev. D**62**, 015008 (2000).
- [31] G 't Hooft and M. Veltman, Nucl. Phys. B**44**, 189(1972); A. Denner, Fortschr. Phys. **41**, 307(1993).